https://doi.org/10.3311/PPci.22681



**Periodica Polytechnica Civil Engineering**, 68(1), pp. 185–196, 2024

# Experimental Analysis of an Innovative Double Strap Joint Splicing of GFRP Bars by NSM Methods for Strengthening RC Beams

Slobodan Ranković[1*], Radomir Folić[2], Andrija Zorić[1], Todor Vacev[1], Žarko Petrović[1], Dušan Kovačević[2]

[1] Faculty of Civil Engineering and Architecture, University of Niš, 14 Aleksandra Medvedeva, 18000 Niš, Republic of Serbia
[2] Faculty of Technical Sciences, Department of Civil Engineering, University of Novi Sad, 21000 Novi Sad, Republic of Serbia
[*] Corresponding author, e-mail: slobodan.rankovic@gaf.ni.ac.rs

Received: 29 May 2022, Accepted: 07 September 2023, Published online: 18 September 2023

**Abstract**

The double strap joint splicing of glass fiber reinforced polymer (GFRP) bars for reinforced concrete (RC) beams strengthening, applying the near surface mounting (NSM) method, has been proposed in the paper. The proposed method consists of application of the supplementary GFRP bars symmetrically positioned in the cut-off zone of the main GFRP reinforcement. The performances of this splicing method have been experimentally tested for the most unfavorable case of the GFRP reinforcement cut-off in the maximal bending moment zones. During the experiment, the varied parameter has been overlapping length of the bars, taking values of 20∅ and 40∅. Evaluation of the splicing technique is done comparing the experimental results with the results of the behavior of beams strengthened by GFRP bars without cut-off and with cut-off, but without splicing. Experimental research encompassed analysis of strength, stiffness, ductility, crack pattern, strains in the steel, GFRP reinforcement and concrete, and the failure modes of the beams. It has been shown that in case of the cut-off of the GFRP bar, strengthening effectivity decreases for 39%, and that in the case of bypassing the cut-off using double strap 20∅ and 40∅ long, strengthening effectivity decreased 23%, and 14% respectively, compared to the beam without GFRP bar cut-off. Using extrapolation, it has been shown that double strap with length of 60∅ provided strength equivalent to the case without cut-off. The result of application of this splicing method of the additional GFRP bars is significant increase of strength and serviceability of the strengthened RC beams.

**Keywords**

RC beams, experimental analysis, NSM GFRP strengthening, reinforcement splicing, double strap joint

## 1 Introduction

One of the contemporary and very efficient techniques for repairing and strengthening of RC structures is application of composite Fiber Reinforced Polymer (FRP) materials as supplementary reinforcement. Within the FRP methods of strengthening, application of the Near Surface Mounting (NSM) method in reinforced concrete (RC) structures takes more and more wide practical use [1–3]. Beside bending and shear strengthening of the RC beams [4, 5], the FRP reinforcement and NSM strengthening method have also found application in the RC slabs strengthening [6, 7]. It is worth mentioning that FRP bars have been mostly used for strengthening, while the application of FRP bars as main reinforcement is protracted due to the lack of available curved reinforcing elements [8].

Compared to the longer standing method of externally bonded laminates (EB-FRP) [9, 10], this technique has some significant advantages, especially regarding better adhesiveness, which directly improves the mechanical characteristics of the strengthened beams [11–14].

The factors that influence the adhesiveness (bond effect) are numerous, and the final strength of the NSM FRP strengthening system mainly depends on the bond effect, considering that different modes of beam failure can occur [15–17]. One of the factors is the length of the FRP bar for strengthening, which is reflected in the failure mode due to the pull-out of the rod in the case when the rod is longer than the cracked span, and due to the peeling-off of the concrete cover in the case when the cracks

**Cite this article as:** Ranković S., Folić R., Zorić A., Vacev T., Petrović, Ž, Kovačević D. "Experimental Analysis of an Innovative Double Strap Joint Splicing of GFRP Bars by NSM Methods for Strengthening RC Beams", Periodica Polytechnica Civil Engineering, 68(1), pp. 185–196, 2024. https://doi.org/10.3311/PPci.22681

reach the end of the FRP rod for strengthening [18]. Other factor that influences the adhesiveness and failure mode of the strengthened beam is surface treatment and the bond effect between the epoxy and the concrete [18, 19]. The type of the FRP reinforcement also has an impact on the strength of the beams. Namely, application of the glass fiber reinforced polymer (GFRP) bars can lead to the failure that occurs in the anchorage zone due to the loss of the bond at the concrete-epoxy interface, while application of the carbon fiber reinforced polymer (CFRP) could provoke failure due to the loss of the bond between the CFRP bar and the surrounding epoxy [20]. The comprehensive state-of-the-art review of the influence of the different parameters on the bond effect has been presented in [21], where FRP texture surface and cross-section geometry, groove surface and geometry, as well as concrete quality, dominantly affect the bond effect. It is remarked that rough surfaces of the FRP bars provide better adhesiveness compared to the smooth surfaces, which also stands for the groove surface. Likewise, the diameter of the FRP bars or width of the rectangular cross-sections of the FRP directly influence the pullout force. The groove dimensions could have positive impact on the bond effect if the failure mode would cohesive at the epoxy, but negative impact on the FRP/epoxy strength if the failure mode were at the interface between epoxy and concrete [21]. As expected, concrete quality reflected in concrete compressive strength, directly influenced the bond effect, but only up to the threshold value when failure mode changes from cohesive one within concrete to another mode type [21].

Since the codes that cover this matter [22–27] are still on the recommendation level and being continuously developed, the research field is open for many issues, and one of them is splicing of the NSM FRP reinforcement.

The problem of splicing of the supplementary NSM FRP reinforcement in the tension zone at RC beams loaded predominantly by bending occurs quite often, considering the limited delivery length of the FRP bars. The standard delivery length of the FRP bars (for diameters greater than ∅10 mm) is 10 m [28], (similarly to the steel bars). Splicing of the NSM FRP reinforcement is a significant issue. Therefore, there is a need for the appropriate solution of this problem in order to provide wide application of this method in every-day engineering practices.

Classical way of splicing for this type of reinforcement by overlapping (slip splices), like the steel reinforcement, has some disadvantages because of unweldability of the FRP composites and asymmetrical disposition. As a variant solution, splicing of the cut-off of the FRP bars can be done by special mechanical devices (Coupler system) using steel or FRP tubes filled with cement paste or epoxy glue (bar splice connections) [29]. Frontal joining is possible using a sleeve connector, by wrapping the FRP with fabric (wrapped tube) [30], but this procedure is impractical because of the limited depth of the cutting in the concrete and pronounced anisotropy of the FRP reinforcement.

To our best knowledge, the results of direct experimental research of the influence of the splicing length of the NSM FRP reinforcement on failure of the strengthened RC beams loaded by bending have not been published.

Previous research has primarily been related to the required anchoring length, which depends on numerous parameters and is determined by bond effect. Most often, laboratory standard samples have been examined, and the adhesiveness of the FRP reinforcement within the concrete has been determined using one of the following test setups: single-shear pushing test; single-shear pulling test; double-shear pushing test; double-shear pulling test; beam-bending test [31]. Results of such examinations can hardly be connected with the behavior of the FRP bars in the structural elements exposed to bending [32–34]. In some research [35], problems of the classic splicing of the NSM FRP have been treated numerically with varying of the overlapping length and groove configuration, and validation of those FE models has been done based on the experimental data from the literature [36], concerning the NSM FRP reinforcement without cut-off. The conclusion was that the overlapping length must be greater than 110 times the bar diameter. All of this indicates that there is a lack of experimental results regarding mechanical characteristics of the real models of the beams loaded predominantly by bending, with different variants of splicing of NSM FRP bars.

Within the presented research [37], the beams strengthened by NSM GFRP reinforcement are treated for the most unfavorable case, i.e., setting the GFRP reinforcement splice in the zone of the maximal bending moments (in this case at the midspan).

In the following text, a proposition of one feasible way of splicing of cut-off of the FRP bars within the NSM strengthening technique called "Double strap joint" method, and experimental results of the mechanical properties of the tested beams strengthened by GFRP bars with diameter of ∅10 mm [28] is presented. The aim of research is establishing of a new method of treatment of the cut-off of NSM FRP reinforcement by both-sided bypassing

(double strap), i.e., using supplements of FRP bars with defined length. Such proposed splicing method would be practical from the engineering aspect, and its advantage over conventional splices is reflected in the symmetrical solution and load transfer in the bar cut-off zone. Also, the aim of this paper is to fill the research gap regarding the limited experimental research of the influence of the splicing length on the strengthened beams performances.

Behavior of RC simply supported beams has been examined using four-point load scheme. The beams were strengthened applying the spirally wound round GFRP bars (rough surface and spiral thread), with and without cut-off, as well as the effects of cut-off bypassing with supplements of various length. Total of five different cases of beams have been examined under test load. Thereat, deflection values, strains in the reinforcement (primary steel bars and additional GFRP bars), strains in concrete, crack pattern and propagation, and failure modes have been registered.

## 2 Configuration of the proposed splice of the NSM FRP

As proposed, bypassing of the FRP reinforcement cut-off is achieved with supplements made of the material identical to the FRP bar, and set in the horizontal concrete cover plane (Fig. 1(a)). The procedure of installing is simple, fast, and efficient enough. It consists of the following steps: a) in the FRP cut-off zone, inside the concrete cover, the existing groove is widened (Fig. 1(b)); b) the FRP supplements are set into the groove; c) connection of the supplements with the cut-off FRP bars is secured by adhesion, using epoxy paste (Figs. 1(c)–(d)); d) connection with the surrounding (basic) concrete is strengthened applying the so-called "primer". The supplements are set both-sided symmetrically, and their length has been varied (20∅ and 40∅). The lengths of the supplement bars have been adopted in a way to be smaller than the recommended overlapping length in the case of classic splicing of the NSM FRP, since it is expected that the double strap will provide better effects. For the purpose of comparison, the case without any supplements has been considered too, as well as the cases of a beam without FRP strengthening (control beam) and the beam with FRP strengthening without

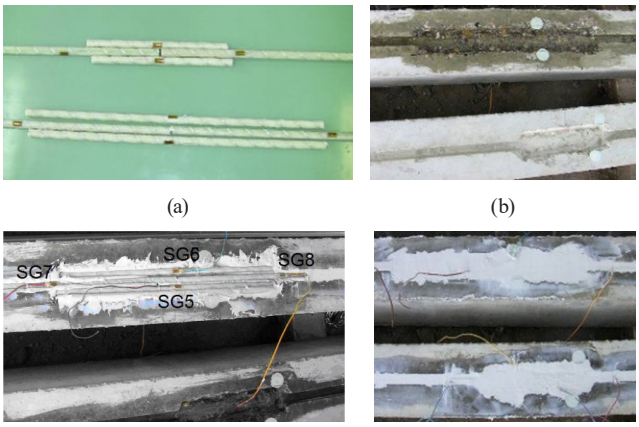


(a) (b) (c) (d)

**Fig. 1** "Double strap joint" method: (a) supplement GFRP reinforcements, (b) groove, (c) installed supplement reinforcement with strain gages (SG5–SG8), (d) double strap joint filled with epoxy

cut-off. The selected width of the groove in the splice zone was 50 mm, and it was wide enough for the epoxy paste to wrap the bars all around by 5 mm, which was in accordance with recommendations [2, 22]. Figs. 1(c)–(d) present disposition of the supplements and setting of the strain gages (SG5–SG8) for controlling the intensity of the force at the FRP cut-off location.

## 3 Experimental program

### 3.1 Material properties

The RC beams were made of concrete with the 28-day cube strength of 31.6 MPa and the steel reinforcement had the yielding strength of $f_{yk}$ = 400 MPa [37]. The commercially available GFRP bars used as NSM reinforcement were Maperod G ∅10 (spirally wound round glass bars), while the MapeWrap11 epoxy and Mapewrap Primer 1 were used as the bonding mortar with the adhesion strength of 3 MPa [28]. The mechanical properties of all materials were experimentally determined before the tests, and they are presented in Table 1.

### 3.2 Experimental setup and procedure

For the purpose of determining the strengthening effects applying the NSM method with and without cut-off of the GFRP reinforcement, experimental tests have been

**Table 1** Material properties

| Material | Diameter [mm] | Elastic modulus [GPa] | Tensile failure strain $\varepsilon \times 1^{0-6}$ | Material strength [MPa] | Manufacturer's data | |
|---|---|---|---|---|---|---|
| | | | | | E [GPa] | fu [MPa] |
| GFRP | ∅10 | 47.0 | 15635 | 735 | 40.8 | 760 |
| Concrete | / | 32.8 | 1220 | 31.6 | / | / |
| Steel bars | ∅12 | 205.0 | 17200 | 400 (560) | / | / |

conducted on samples with disposition and geometry as presented in Fig. 2. The RC beams strengthened by GFRP reinforcement were loaded by concentrated forces in the thirds of the span according to the four-point load scheme.

The beams with the cut-off of the NSM GFRP in the midspan, i.e., in the zone of the maximal bending moments, have been examined as the most unfavorable case, and compared with the results of behavior of the beams with continually set GFRP reinforcement, and with the unstrengthen beam. The length of the "bypassing" has been varied during research. The bypassing of the cut-off of the GFRP bar has been done by symmetric setting of supplements, made of the same material and same diameter (∅10), with lengths of 20 cm (20∅) and 40 cm (40∅),

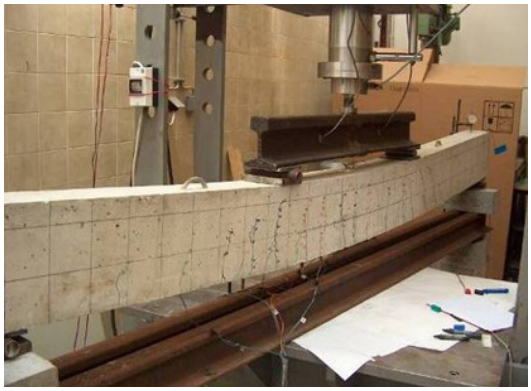

(a)

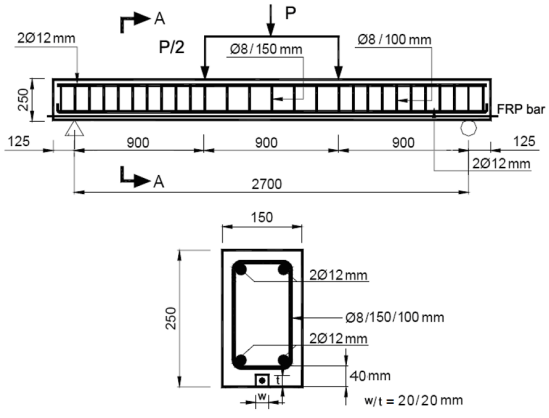


(b)

**Fig. 2** Experimental setup: (a) view, (b) structural details

respectively. The labels of the experimental samples and variants of the splices of the NSM GFRP reinforcement cut-off are presented in Table 2.

During the test, the following parameters, expressed as a function of load, have been registered: deflection, strains in the steel and GFRP reinforcement, strains in concrete, crack pattern and propagation, as well as the failure modes. Load disposition of the samples and setting of the measuring points, as well as setup of the measurement equipment during the test, are presented in Fig. 3, for the beam with bypassing of the NSM FRP cut-off by overlapping of 40∅.

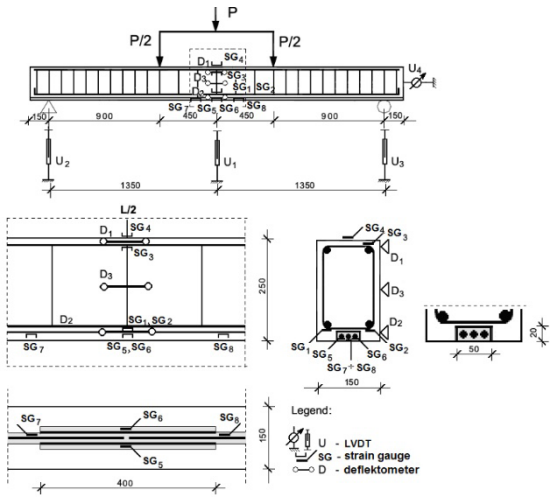


(a)

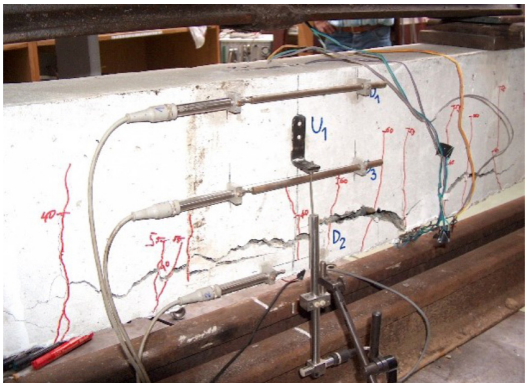


(b)

**Fig. 3** Instrument setting: (a) scheme of the beam with cut-off of the GFRP reinforcement and supplements of 40∅ (B-G4), (b) setup of the sample during the test

**Table 2** Labels and characteristics of the tested samples

| Beam label | Main GFRP reinforcement | Used main and "double strap joint" GFRP reinforcement | |
|---|---|---|---|
| 1 | B-con | / | / |
| 2 | B-G1 | NSM GFRP | 1∅10 l = 300 cm (continually along the whole span) |
| 3 | B-G2 | NSM GFRP | 1∅10 l = 150 cm + 150 cm (cut-off at L/2, without continuity of cut-off) |
| 4 | B-G3 | NSM GFRP | 1∅10 l = 150 cm + 150 cm (cut-off at L/2) + 2∅10, 20 cm (20∅) |
| 3 | B-G4 | NSM GFRP | 1∅10 l = 150 cm + 150 cm (cut-off at L/2) + 2∅10, 40 cm (40∅) |

### 3.3 Test instrumentation and measuring devices

The samples have been tested in the test device with load capacity of 1000 kN, with continual applying of load by hydraulic press. The test was in the "displacement control mode" with constant grow rate of deflection set as 0.02 mm/s, up to failure. The range of load measuring cell was up to 100 kN. Deflection was measured by linear variable displacement transducers (LVDT). The strains in concrete, as well as in the steel and GFRP reinforcement, have been registered using the strain gauges with base of 100 mm and 6 mm, respectively. It was not possible to measure the width of an individual crack using the available LVDT, so the summed width of all cracks that appear on the base length of the LVDT, which is 100 mm, has been measured. All data have been acquired via the data acquisition system, with an automatic data reading period of 1 s.

## 4 Test results and comparative analysis

### 4.1 Deflection and load capacity analysis

Efficiency of the splice of the GFRP bars is presented through the analysis of the load-deflection and load-strain dependence. From the load-deflection diagram (Fig. 4), one may observe that cut-off of the GFRP reinforcement and the bypassing length significantly affect beam strength and deformations at failure. At low load levels, up to the steel reinforcement yield, that is, up to deflection of ≈ 10 mm (L/270), the beam stiffness is little affected by GFRP strengthening, regardless of the presence/absence of the cut-off, and independently of the bypassing length. At higher load levels, failure occurs because of the crack propagation in the tension zone and stiffness decrease, which is especially prominent at beams B-G2, and B-con. This is in fact justification of the idea of the need for splicing of the cut-off of the FRP reinforcement with bypassing, wherewith an increase of the efficiency of the method is achieved (B-G3 and B-G4). One may observe an almost identical behavior regarding the stiffness of the strengthened beams (load-deflection relation), with a remark that strength is decreased with the decrease of the bypassing length.

Fig. 5(a) presents absolute strength [kN], and Fig. 5(b) relative strength [%] of the tested beams. One may see that strength of the beam without bypassing (B-G2) is 61 % compared to the beam without cut-off of the NSM GFRP reinforcement, whose strength is denoted as 100%.

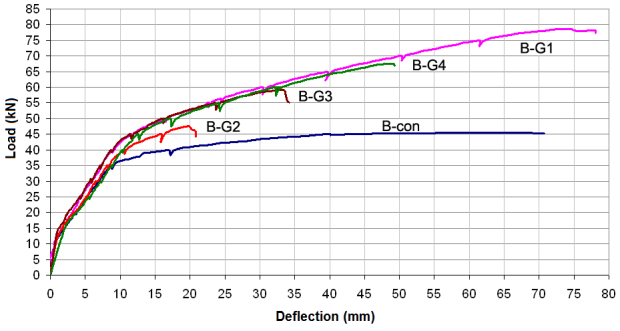


**Fig. 4** Load-deflection diagrams for different variants of splicing of GFRP reinforcement

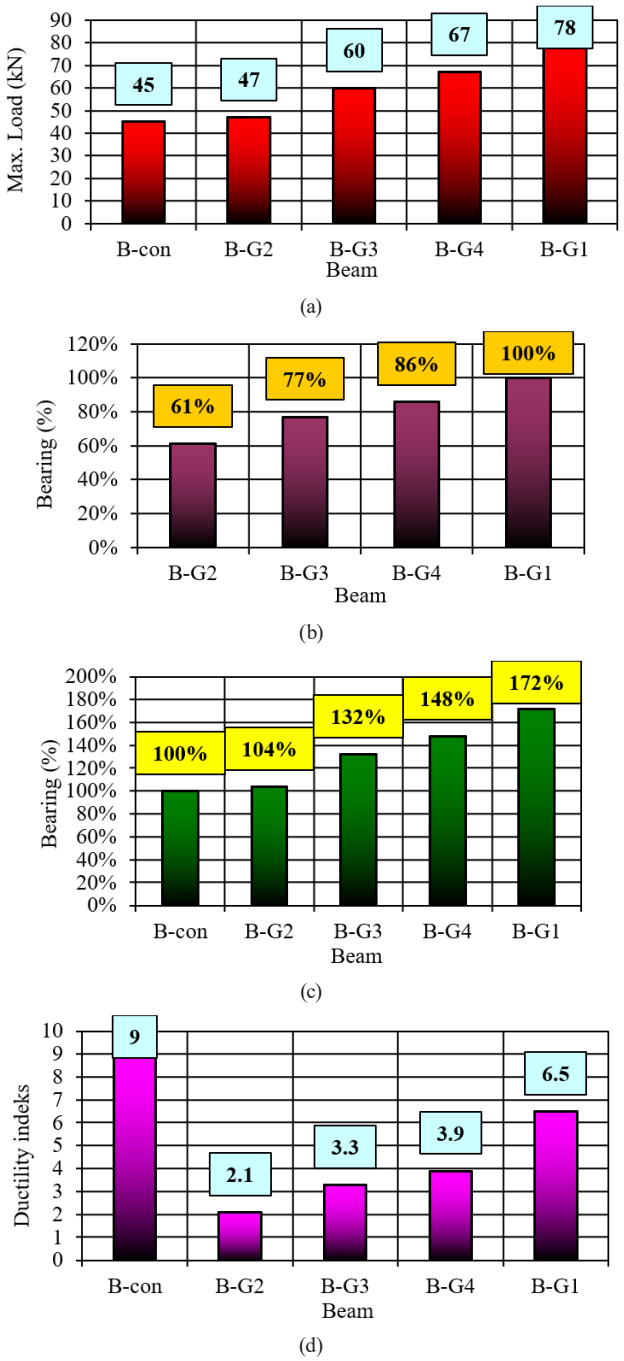


**Fig. 5** Strength and ductility of the tested specimens: (a) max. strength, (b) strength related to the B-G1 (%), (c) strength related to the B-con (%), (d) ductility index

If bypassing with length 20∅, that is, 40∅ (beams B-G3 and B-G4) is added, the strength is 77%, and 86%, respectively, compared to the beam without cut-off of GFRP (B-G1). This is a good indication of the efficiency of the proposed technique for cut-off treatment.

Diagram in Fig. 5(c) presents strength of the beams with application of the NSM FRP strengthening compared to the non-strengthened beam B-con, whose strength is taken as referent, i.e., 100%. In the case of beam strengthening with GFRP reinforcement with cut-off and without bypassing (B-G2), strength is only 104%. In the case of bypassing with length 20∅ (B-G3), that is, 40∅ (B-G4), strength is 132% and 148%, respectively, while the beam without GFRP bar cut-off (B-G1) has strength of 172%, compared to the non-strengthened beam (B-con).

Increase of the ductility index due to the increase of the bypassing length is presented in Fig. 5(d). The ductility index (DI) ranges from 2.1 to 6.5, so one may indirectly conclude that for the minimal required value (DI > 4), the minimal length of the added supplements should be greater than 40∅.

The experimental result of the load-deflection response of the RC beam strengthened with GFRP bar without cut-off (B-G1) is compared to the well-known analytical model. The midspan deflection (Δ) of rectangular beam subjected to four-point load can be calculated using following expression [38]:

$$\Delta = \frac{23PL^3}{1296EI} + \frac{k_s PL}{6GA}, \tag{1}$$

where:

$P$ is the load intensity,

$L$ = 2700 mm is the beam span,

$k_s$ = 6/5 is the shear correction factor for rectangular cross sections,

$E$ is the modulus of elasticity of concrete (Table 1),

$G = E/2(1 + \nu) = 32.8/2(1 + 0.2) = 13.67$ GPa is the shear modulus of concrete.

Geometrical properties in the Eq. (1) should be calculated for transformed section regarding the concrete material. The load-deflection response of RC beam can be separated into three linear branches: pre-cracked, pre-yield and post-yield. The first branch is characterized with uncracked concrete where applied bending moment ($M$) is lower than cracking moment ($M_{cr}$). For this calculation the gross moment of inertia of the cross-section ($I$) is used in the Eq. (1). The second branch is characterized with the occurrence of the cracks in the concrete. In order to consider the loss of stiffness due to concrete cracking, the effective moment ($I_e$) of inertia of the cross-section should be used in the Eq. (1), which can be obtained by [39]:

$$I_e = \frac{I_{cr}}{1-\gamma\left(\frac{M_{cr}}{M}\right)^2\left[1-\frac{I_{cr}}{I}\right]} \le I, \tag{2}$$

where factor $\gamma = 1.72 - 0.72(M_{cr}/M)$ accounts for the length of the uncracked regions of the RC beam.

The detailed procedure for estimation of the geometrical characteristics of the RC cross-section in the pre-cracked ($I$) and pre-yield phases ($I_{cr}$), as well as for estimation of cracking ($M_{cr}$) and yielding moment ($M_y$), is not presented for the consistency of the presentation, but the reader is referred to the reference [38]. It is worth mentioning that in the post-yield branch the tangent modulus of steel reinforcement is used for calculation of transformed cross-section properties in order to cover yield of the steel bars.

The comparation of the experimentally and analytically obtained load-deflection dependence of the B-G1 model is presented in the Fig. 6. It can be concluded that analytical approach predicts satisfactorily the deflection of the beam in the first and the second branch (up to the yield of the steel bars). Some deviation of the analytical solution is present after the yielding of the steel bars. Namely, analytical approach provides slightly stiffer prediction compared to the experimental results, where ultimate deflection is underestimated for approximately 20%. This result is in accordance with the results of other researchers [38], and confirms the need to develop a more adequate analytical model for load-deflection response of the RC beam strengthened with GFRP bar after steel reinforcement yielding.

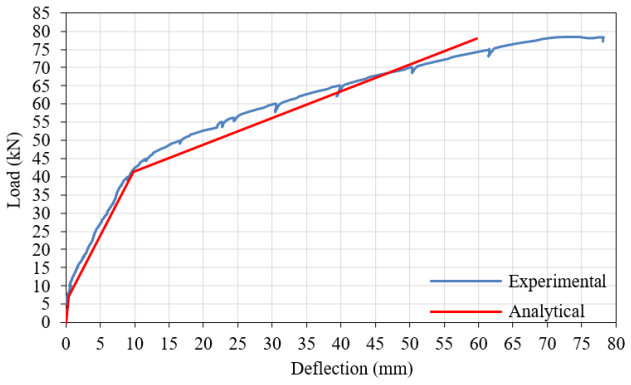


**Fig. 6** Experimental and analytical load-deflection diagrams for B-G1

#### 4.1.1 Defining of the required splicing length based on approximative function

Based on the experimental results (Fig. 5(c)), and the obtained dependence between the splicing length of the cut-off and percentual strength regarding the unstrengthen beam, a linear approximate function has been derived, by which one may roughly determine the required bypassing length, so that splicing achieves strength equal to the bars without cut-off.

Applying the method of the least squares [40], an approximate function has been obtained:

$$\phi(x) = 106 + 1.1 \times x\,. \tag{3}$$

Using that function, and the percent of strength achieved by the GFRP reinforcement without cut-off (172%):

$$\phi(x) = 172\,, \tag{4}$$

one obtains the overlapping length $x$ = 60 cm, which is required to achieve the beam strength without cut-off of the GFRP reinforcement.

Fig. 7 presents the approximate function obtained from the experimental data given in Fig. 5(c) and based on the Eqs. (3) and (4).

This leads to the conclusion that strength decrease will not occur at beams with spliced GFRP reinforcement if its cut-off is spliced with "double strap joint" with length of 60∅. It is worth mentioning that this conclusion needs to be supported by much prominent experimental research or by the comprehensive numerical analysis in the further research.

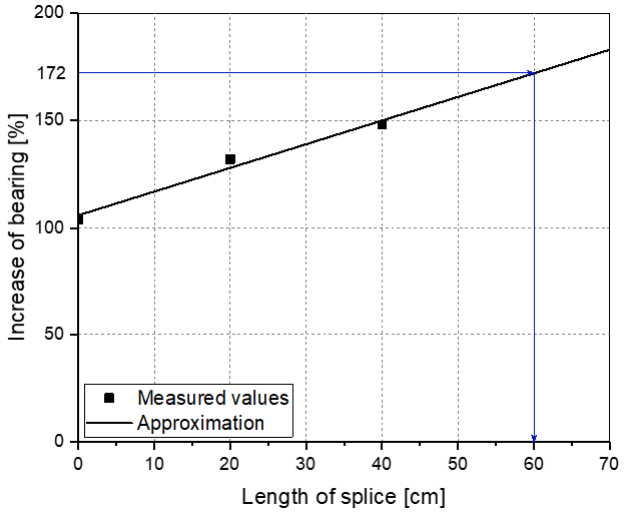


**Fig. 7** Strength increase vs. splicing length

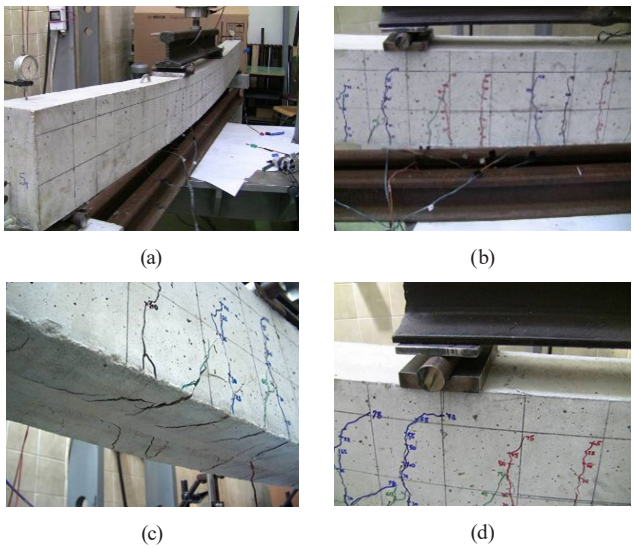


**Fig. 8** (a) B-G1, beam deflection (Δmax = 78 mm), (b) B-G1, max. crack width ($\delta$max = 3.2 mm), (c) B-G1, beam failure caused by the loss of concrete-epoxy connection, (d) B-G1, beam concrete crushing in the area of force application at the beam failure

### 4.2 Failure modes and load capacity

#### 4.2.1 Beam without cut-off of the GFRP reinforcement (B-G1)

The deflection of the B-G1 beam [20] is shown in Fig. 8(a), and the typical crack pattern in Fig. 8(b). The beam strengthened with the GFRP reinforcement and its failure mechanism under the test load are shown in Figs. 8(c) and 8(d). One may see that the beam is highly deformable and with very good ductility, that the crack pattern is uniform, and that the failure is caused by the exceeding tensile stress on the concrete-epoxy interface in the groove. Transverse cracks on the bottom side of the beam do not intersect with the groove containing the strengthening and the epoxy filling because it has higher tensile strength compared to concrete; instead, they run along the concrete-epoxy interface (Fig. 8(c)). These cracks arise after the occurring of steel reinforcement yield, they propagate at approx. angle of 45° across the beam width (Fig. 8(c)). Due to the surface roughness of the GFRP reinforcement, the loss of adhesion at the epoxy bond failed to occur. At higher loads, concrete crushing occurs at force application points around the steel plate that transfers the load onto the beam (Fig. 8(d)).

#### 4.2.2 Beams with cut-off of the GFRP reinforcement (B-G2, B-G3, B-G4)

Failure of the beams with cut-off of the NSM GFRP reinforcement, with or without the cut-off bypassing, has its specificities regarding the failure mode. An abrupt development of one dominant crack occurs at beam without cut-off bypassing (B-G2), at the location of the cut-off of

the GFRP reinforcement, which rapidly propagates with the load increase (Fig. 9), finally exhibiting very small strengthening effect (only 4%). Adding the double strap joint at the cut off of the bar (B-G3 and B-G4) causes the relocation of the failure into the zone of the bypassing ending, and the concrete peeling-off occurs along the depth of the cover (Fig. 10). The crack pattern is more uniform, and the behavior of the beam is more ductile for longer bypassing. The tension force is transferred from the GFRP reinforcement through the epoxy glue onto the concrete, in which an exceeding of the tension stresses and concrete peeling-off occurs at one end of the bypassing bars. Therefore, concrete peeling-off in longitudinal sense occurs at the epoxy-concrete contact, which is at the beginning of the groove widening for inserting the additional bars (Fig. 11). It is worth mentioning that all beams with cut-off of the GFRP bar, after reaching the ultimate load and after reaching the failure of GFRP strengthening, behave as the control beam, considering the same steel reinforcement. This branch is not presented in the load-deflection diagrams (Fig. 4) for the purpose of presentation clarity, and besides that, it is not decisive for the assessment of the influence of the double strap join splicing of the GFRP cut-off on the bearing capacity of the beams.

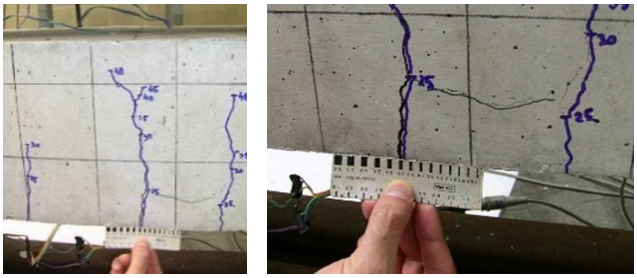

(a) (b)

**Fig. 9** Crack pattern at the beam B-G2 (cut off, without bypassing), dominant crack at the cut off: (a) general view, (b) detail view

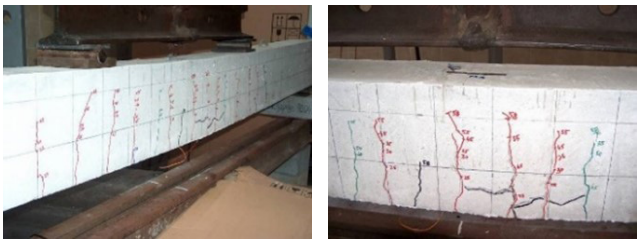

(a) (b)

**Fig. 10** Crack distribution at beam B-G3 (bypassing 20∅): (a) general view, (b) detail view

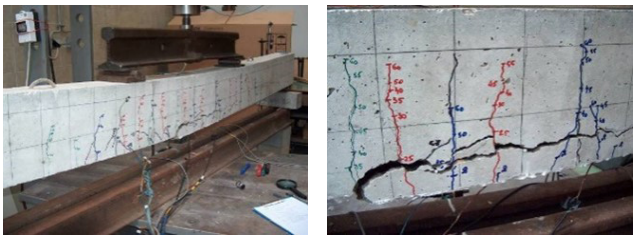

(a) (b)

**Fig. 11** Crack distribution at beam B-G4 (bypassing 40∅): (a) general view, (b) detail view

### 4.3 Analysis of the crack patterns in concrete

The crack width has been measured as a function of load intensity in two ways. Firstly, summed crack width has been measured using LVDT with measuring base of 100 mm in the beam midspan, continually at every second. Secondly, single cracks have been measured using the crack meter (ZDI-VDA) at every 5 kN of load increment. Comparative diagrams of the crack widths using LVDT gauge for all tested beam specimens are given in Fig. 12.

One may observe favorable influence of the increase of the bypassing length regarding the serviceability of the beam, that is, the crack pattern. The differences become more prominent starting from steel reinforcement yield (approx. load level 35 kN) up to the beam failure. Tension strains in the concrete are here neglected, considering the fact that elastic part of the diagram ends for the crack width lower than 0.05 mm, which can be seen in the diagram in Fig. 12. Such approach enables continual tracking of the cracks, because acquisition is done at every second, and the simplifications are minimal.

In quantitative sense, arise and development of the cracks shows that there is no big difference regarding the bypassing length of the GFRP up to the steel reinforcement yield, that is, up to the crack width of approx. $\delta = 0.3$ mm. With further load increase, depending on the bypassing length of the GFRP cut-off, the load level at which certain crack width occurs, also rises. This is in accordance with the strength increase of the beams due to the increase of the bypassing length as well.

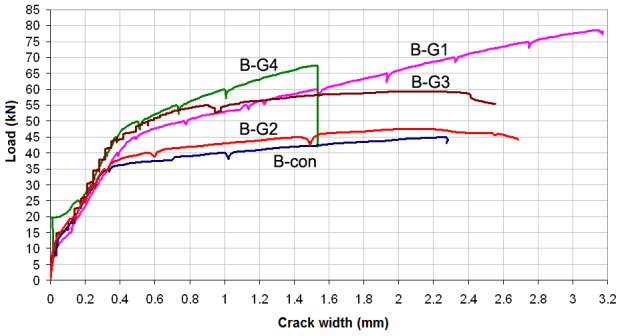


**Fig. 12** Crack width diagrams for all tested beam specimens

Based on the "crack maps", Fig. 13, one may predict progression and development of the cracks for different load levels (I phase - red, II phase - blue, III phase – green, and IV phase - black), for all tested specimens. From the registered load levels, one may note occurrence of the cracks and see their propagation limits. Longitudinal spacing of the cracks in the zone of pure bending is approx. equal to the stirrup spacing (15 cm), for starting load levels, while with the further load increase, they become denser. One may note a qualitative difference in the crack pattern between the beams with cut-off bypassing and the beam with continual (without cut-off) GFRP reinforcement. At beams with bypassed cut-off of the GFRP bars, cracks are first formed out of the zone of bypassing, and after that, an abrupt propagation of cracks arises at the bypassing zone endings. This leads to the concrete peeling-off across the bypassing length. Regarding the beam depth, failure occurs in the concrete cover.

### 4.4 Analysis of strains in concrete

Comparative values of strains at the top fiber of the compressed zone of the concrete in the beam midspan are presented in Fig. 14. One may note decrease of the strain values in the top fiber of the compressed zone of the concrete, if the bypassing of the GFRP reinforcement cut-off is applied. The beam without bypassing (B-G2) has the largest strains for the same load level, because occurring of the dominant crack in the midspan leads to the earlier stiffness decrease of the beam, and to a larger deflection. One characteristic case is the failure caused by the concrete peeling-off in the tensed zone of the protective layer (at the bypassing length of 40∅, beam B-G4), which causes an abrupt decrease of the beam stiffness, after which the compressing strains in concrete rise, and the beam behaves as non-strengthened. Similar situation is at beam with bypassing of 20∅ (B-G3), but with less prominent decrease of stiffness at the moment of failure of the bypassing function.

### 4.5 Analysis of strains in the GFRP reinforcement

A characteristic mechanism of tension force distribution at NSM FRP strengthening with the treated cut-off of the GFRP bar may be seen in Fig. 15. The figure presents strains in the GFRP bar (SG7 and SG8) and in the supplements (SG5 and SG6), for the beam B-G4, with both-sided overlapping 40∅ long.

One may see from the diagram that strains in the supplements for splice bypassing (SG5 and SG6) completely follow the strains in the longitudinal GFRP bar (SG7 and SG8) up to the load of 30 kN. With further load increase, a difference in strain values occurs, so that greater part of the stresses, i.e., tension force, takes the NSM GFRP bar, and the supplement fails at approx. load level of 55 kN. Maximal strains in the basic GFRP bar are multiply higher compared to the supplementary GFRP bars at beam failure. A similar qualitative stress-strain state also occurs for overlapping of 20∅, but with lower nominal values of strains at same load level.

Diagrams in Fig. 16 present comparative values of the strains in the GFRP reinforcement in the midspan. It is worth mentioning that measuring spot SG5 was in the supplementary bars for cut-off bypassing at the beams B-G3

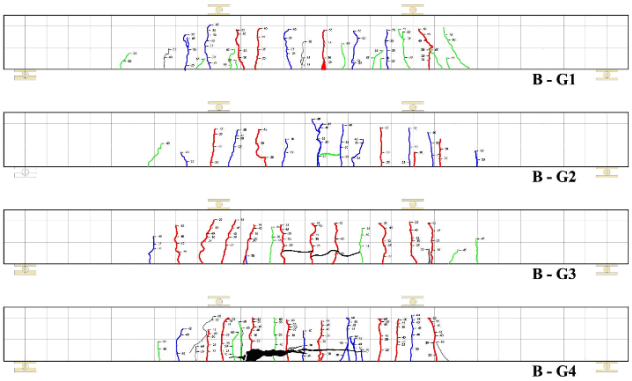


**Fig. 13** Crack pattern for different bypassing lengths of cut-off through load phases

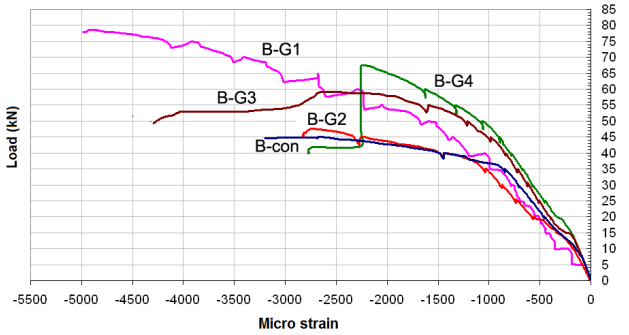


**Fig. 14** Strains in the top compressed concrete fiber (SG4), as a function of bypassing length

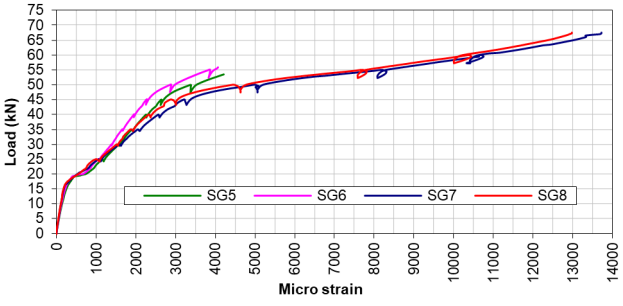


**Fig. 15** Strains in the GFRP reinforcement in the zone of cut-off splicing (B-G4)

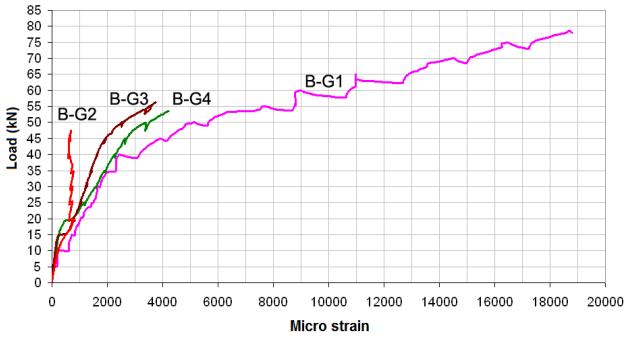


**Fig. 16** Strains in the GFRP reinforcement in the midspan – measuring spot SG5

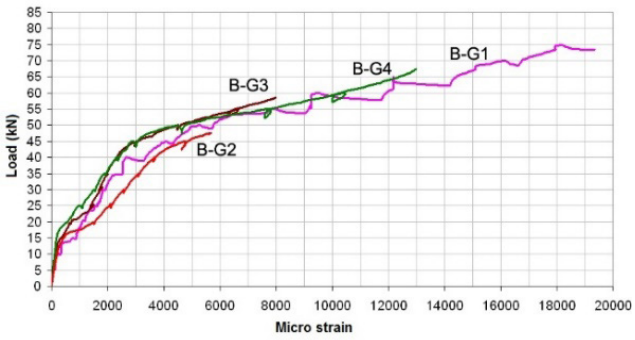


**Fig. 17** Strains in the GFRP reinforcement out of the cut-off zone - measuring spot SG8

and B-G4 (Fig. 3) and in the beams B-G1 and B-G2 without splices, the measuring spot was also in the midspan, but on the main GFRP reinforcement. It has been noted that greater length of bypassing causes redistribution of stresses: share of the bypassing in the tension force transfer becomes more significant, and strains in the bypassing bars increase. Strains in the beam without bypassing (B-G2) at the location of cut-off are minimal, because slipping of the GFRP bar occurs. In the case of the bypassing length of 20∅ (B-G3) and 40∅ (B-G4), supplementary bars take larger part of the load at the cut-off joint. This part is proportional to the bypassing length increase, but still much smaller than in the case of continual strengthening (B-G1). The beam without cut-off of the GFRP reinforcement (B-G1) takes larger part of load by GFRP reinforcement in the midspan. This is reflected in higher strains (stresses) and composite action with remained elements in the cross-section. This means that the tension force is the greatest in the GFRP reinforcement without cut-off, and the lowest in the disrupted GFRP bar without overlapping by bypassing. By adding the supplements, tension force is transferred from the base NSM GFRP bar via the epoxy glue onto the supplements and increases with the increase of their length.

Fig. 17 presents diagrams of strains vs. load in the NSM GFRP reinforcement out of the bypassing zone (measuring spot SG8). One may observe lower strains for the same load level at the beams with bypassing, as well as an almost equal load transfer at beams B-G3 and B-G4 up to failure, which arises at different load levels. At the beam without bypassing (B-G2), more prominent strains in the GFRP bar and occurrence of earlier failure are noted. This is a consequence of forming an additional crack in the midspan, which causes decrease of stiffness and increase of deflection. Similar result has been obtained in the case of the beam B-G3, too.

## 5 Conclusions

A new technique of splicing of FRP reinforcement made of round bars at NSM system for strengthening of the beams in the bending zone, called "Double strap joint" NSM FRP, has been proposed in the paper. Experimental research indicates the need and significance for providing continuity of the GFRP reinforcement for strengthening in the NSM method, and the obtained results confirmed efficiency of the proposed splicing solution.

Besides the practical advantages that are reflected in the symmetry of the solution and simple technological preparation and realization, prominent structural advantages of this method are also present, and they can be summarized as:

- Application of strengthening by NSM GFRP bar ∅10 mm results with the ultimate strength increases for 73%, while in the case of cut-off without bypassing, this increase is only 4%. Introducing the bypassing by both-sided overlapping of 20∅, and 40∅ length, ultimate strength of the beam increases for 32%, and 48% respectively, compared to the unstrengthen beam.
- Elastic stiffness of the beam is little affected by GFRP strengthening, while its post-elastic stiffness is larger than the post-elastic stiffness of the unstrengthen beam. The bypassing length has no influence on the beam stiffness, but on the strength.
- The RC beam strengthened by NSM GFRP reinforcement with cut-off in the midspan shows failure due to a dominant crack at the cut-off location. In the case of bypassing ("double strap joint") with 20∅ and 40∅ length, failure occurs by concrete peeling-off at higher load levels, and at the endings of the supplement grooves. Failure occurs due to the tensile stress exceeding at the epoxy-concrete interface, and in the zone of concrete cover, considering beam depth.

- The crack image indicates "regular" behavior of the tested strengthened beams in the case of "double strap joint" application, which confirms that proposed splicing solution also improves the serviceability of the beam.
- Ductility of the beam also rises with the increase of the length of the cut-off bypassing. Satisfying ductility may be achieved with bypassing length greater than 40∅.
- Based on the measured strains in the NSM GFRP reinforcement and in supplements for cut-off treatment, one may conclude that the tension force is transferred from the NSM GFRP reinforcement onto supplements via epoxy glue, and it increases with the increase of overlapping length.
- Applying the approximative method of the least squares, it has been shown that minimal required bypassing length is 60∅, in order to provide strength equal to the case of strengthening without cut-off.

Conclusion regarding minimal required bypassing length stands for the here examined cases. In order to define some general criteria for the minimal bypassing length, an analysis of numerous parameters would be necessary. Above all, these are: type of the FRP reinforcement, type of epoxy, groove dimensions, concrete class, as well as the possible combinations of those parameters. Results of this research can be especially valuable for the manufacturers of the FRP reinforcement. They can serve as a base for their recommendation for applications of their specific products (bars and its surface treatment, glue, groove preparation etc.).

It may be expected that experimental, analytical, and especially numerical methods contribute to the affirmation of this technique for splicing of the NSM FRP bar reinforcement. Our further research will be directed towards the development of sophisticated numerical model for the analysis of the "double strap joint" splicing method, validated regarding the experimental results. Using such numerical model, the conclusion regarding the required overlapping length in the proposed splicing method will be fully confirmed. Also, numerical analysis could be used for further research of the influence of the different types of the FRP reinforcement on the RC beam performances with application of the innovative "double strap joint" splicing method.

## References

[1] El-Hacha, R., Rizkalla, S. H. "Near-Surface-Mounted Fiber-Reinforced Polymer Reinforcements for Flexural Strengthening of Concrete Structures", ACI Structural Journal, 101(5), pp. 717–726, 2004. https://doi.org/10.14359/13394

[2] De Lorenzis, L., Teng, J. G. "Near-surface mounted FRP reinforcement: An emerging technique for strengthening structures", Composites Part B: Engineering, 38(2), pp. 119–143, 2007. https://doi.org/10.1016/j.compositesb.2006.08.003

[3] Szabó, Z. K., Balázs, G. L. "Near surface mounted FRP reinforcement for strengthening of concrete structures", Periodica Polytechnica Civil Engineering, 51(1), pp. 33–38, 2007. https://doi.org/10.3311/pp.ci.2007-1.05

[4] Jedrzejko, M. J., Zhang, S. S., Ke, Y., Fernando, D., Nie, X. F. "Shear strengthening of RC beams with NSM FRP. I: Review of strength models", Advances in Structural Engineering, 26(3), pp. 564–584, 2023. https://doi.org/10.1177/13694332221125832

[5] Imjai, T., Setkit, M., Garcia, R., Figueiredo, F. P. "Strengthening of damaged low strength concrete beams using PTMS or NSM technique", Case Studies in Construction Materials, 13, e00403, 2020. https://doi.org/10.1016/j.cscm.2020.e00403

[6] Imjai, T., Garcia, R., Kim, B., Hansapinyo, C., Sukontasukkul, P. "Serviceability behaviour of FRP-reinforced slatted slabs made of high-content recycled aggregate concrete", Structures, 51, pp. 1071–1082, 2023. https://doi.org/10.1016/j.istruc.2023.03.075

[7] Foret, G., Limam, O. "Experimental and numerical analysis of RC two-way slabs strengthened with NSM CFRP rods", Construction and Building Materials, 22(10), pp. 2025–2030, 2008. https://doi.org/10.1016/j.conbuildmat.2007.07.027

[8] Imjai, T., Garcia, R., Guadagnini, M., Pilakoutas, K. "Strength Degradation in Curved Fiber-reinforced Polymer (FRP) Bars Used as Concrete Reinforcement", Polymers, 12(8), 1653, 2020. https://doi.org/10.3390/polym12081653

[9] Nanni, A. "North American design guidelines for concrete reinforcement and strengthening using FRP: principles, applications, and unsolved Issues", Construction and Building Materials, 17(6–7), pp. 439–446, 2003. https://doi.org/10.1016/S0950-0618(03)00042-4

[10] Wattanapanich, C., Imjai, T., Garcia, R., Rahim, N. L., Abdullah, M. M. A. B., Sandu, A. V., Vizureanu, P., Matasaru, P. D., Thomas, B. S. "Computer Simulations of End-Tapering Anchorages of EBR FRP-Strengthened Prestressed Concrete Slabs at Service Conditions", Materials, 16(2), 851, 2023. https://doi.org/10.3390/ma16020851

[11] Hassan, T. K., Rizkalla, S. H. "Bond Mechanism of Near-Surface-Mounted Fiber-Reinforced Polymer Bars for Flexural Strengthening of Concrete Structures", ACI Structural Journal, 101(6), pp. 830–839, 2004. https://doi.org/10.14359/13458

[12] Täljsten, B., Carolin, A, Nordin, H. "Concrete structures strengthened with near surface mounted reinforcement of CFRP", Advances in Structural Engineering, 6(3), pp. 201–213, 2003. https://doi.org/10.1260/136943303322419223

[13] Teng, J. G., De Lorenzis, L., Wang, B., Li, R., Wong, T. N., Lam L. "Debonding failures of RC beams strengthened with near-surface mounted CFRP strips", Journal of Composites for Construction, 10(2), pp. 92–105, 2006. https://doi.org/10.1061/(ASCE)1090-0268(2006)10:2(92)

[14] Al-Mahmoud, F., Castel, A., François, R. "Failure modes and failure mechanisms of RC members strengthened by NSM CFRP composites – Analysis of pull-out failure mode", Composites Part B: Engineering, 43(4), pp. 1893–1901, 2012. https://doi.org/10.1016/j.compositesb.2012.01.020

[15] Thiagarajan, G. "Experimental and Analytical Behavior of Carbon Fiber-Based Rods as Flexural Reinforcement", Journal of Composites for Construction, 7(1), pp. 64–72, 2003. https://doi.org/10.1061/(ASCE)1090-0268(2003)7:1(64)

[16] Carolin, A., Nordin, H., Täljsten, B. "Concrete beams strengthened with near surface mounted reinforcement of CFRP", In: Teng J.-G. (ed.) International Conference on FRP Composites in Civil Engineering, Volume 2, Hong Kong, China, 2001, pp 1059–1066. ISBN: 0-08-043945-4

[17] Parretti, R., Nanni, A. "Strengthening of RC Members Using Near-Surface Mounted FRP composites: Design Overview", Advances in Structural Engineering, 7(6), pp. 469–483, 2004. https://doi.org/10.1260/1369433042863198

[18] Al-Mahmoud, F., Castel, A., François, R., Tourneur C. "Strengthening of RC members with near-surface mounted CFRP rods", Composite Structures, 91(2), pp. 138–147, 2009. https://doi.org/10.1016/j.compstruct.2009.04.040

[19] Ranković, S., Folić, R., Mijalković, M. "Effects of RC beams reinforcement using near surface reinforced FRP composites", Facta Universitatis Series: Architecture and Civil Engineering, 8(2), pp. 177–185, 2010. https://doi.org/10.2298/FUACE1002177R

[20] Ranković, S., Folić, R., Mijalković, M. "Flexural behaviour of RC beams strengthened with NSM CFRP and GFRP bars – experimental and numerical study", Romanian Journal of Materials, 43 (4), pp. 377–390, 2013.

[21] Coelho, M. R. F., Sena-Cruz, J. M., Neves, L. A. C. "A review on the bond behavior of FRP NSM systems in concrete", Construction and Building Materials, 93, pp. 1157–1169, 2015. https://doi.org/10.1016/j.conbuildmat.2015.05.010

[22] American Concrete Institute, Committee 440 "Guide for the Design and Construction of Externally Bonded FRP Systems for Strengthening Concrete Structures", Farmington Hills, MI, USA, 2017.

[23] Fédération Internationale du Béton (Fib), Bulletin no. 90 "Externally applied FRP reinforcement for concrete structures". Lausanne, Switzerland, 2019.

[24] Concrete Society, Technical Report 55 "Design guidance for strengthening concrete structures using fibre composite materials", Crowthorne, UK 2012.

[25] ISIS Educational Module 4 "An Introduction to FRP Strengthening of Concrete Structures", A Canadian Network of Centres of Excellence, 2004.

[26] American Concrete Institute, Committee 440 "Guide Test Met-ods for Fiber-Reinforced Polymers (FRPs) for Reinforcing or Strengthening Concrete Structures", Farmington Hills, MI, USA, 2012.

[27] American Concrete Institute, Committee 440 "Guide for the Design and Construction of Structural Concrete Reinforced with Fiber-Reinforced Polymer (FRP) Bars ", Farmington Hills, MI, USA, 2015.

[28] Mapei FRP System, [online] Available at: www.mapei.com

[29] Yuan, G. Q., Zhu, N. "A Review on the Connection of FRP Bars", Applied Mechanics and Materials, 238, pp. 61–65, 2012. https://doi.org/10.4028/www.scientific.net/AMM.238.61

[30] Koushfar, K., Rahman, A. B. A., Ahmad, Y. "Bond behavior of the reinforcement bar in glass fiber-reinforced polymer connector", Građevinar, 66(4), pp. 301–310, 2014. https://doi.org/10.14256/JCE.913.2013

[31] Bilotta, A., Ceroni, F., Barros, J. A. O., Costa, I., Palmieri, A., Szabó Z. K., Nigro, E., Matthys, S., Balazs, G., Pecce, M. "Bond of NSM FRP-Strengthened Concrete: Round Robin Test Initiative", Journal of Composites for Construction, 20(1), 4015026, 2016. https://doi.org/10.1061/(ASCE)CC.1943-5614.0000579

[32] Zhou, J., Stümpel, M., Kang, C., Marx, S. "Lap-spliced connections of steel and FRP bars in reinforced flexure concrete structures", Engineering Structures, 263, 114409, 2022, https://doi.org/10.1016/j.engstruct.2022.114409

[33] Mousavi, S. R., Sohrabi, M. R., Moodi, Y., Gholamhosseini, E. "Strengthening of Lap-Spliced RC Beams Using Near-Surface Mounting Method", Iranian Journal of Science and Technology - Transactions of Civil Engineering, 46, pp. 251–259, 2022. https://doi.org/10.1007/s40996-020-00577-5

[34] Shadravan, B., Tehrani, F. M. "A Review of Direct Shear Testing Configurations for Bond between Fiber-Reinforced Polymer Sheets on Concrete and Masonry Substrates", Periodica Polytechnica Civil Engineering, 61(4), pp. 740–751, 2017. https://doi.org/10.3311/PPci.9090

[35] Kadhim, M. M. A., Jawdhari, A., Peiris, A. "Evaluation of lap-splices in NSM FRP rods for retrofitting RC members", Structures 30, pp. 877–894, 2021. https://doi.org/10.1016/j.istruc.2021.01.054

[36] De Lorenzis, L. "Strengthening of RC structures with near surface mounted FRP rods", PhD Thesis, Department of Civil Engineering, The University of Lecce, 2002.

[37] Ranković, S. "Eksperimentalno-teorijska analiza graničnih stanja armiranobetonskih linijskih nosača ojačanih sprezanjem sa NSM vlaknastim kompozitima" (Experimental and theoretical limit state analysis of reinforced concrete beams strengthened with NSM fiber composites), PhD Thesis, University of Niš, 2011. (in Serbian)

[38] Imjai, T., Setkit, M., Figueiredo, F. P., Garcia, R., Sae-Long, W., Limkatanyu, S. "Experimental and numerical investigation on low-strength RC beams strengthened with side or bottom near surface mounted FRP rods", Structure and Infrastructure Engineering, OnlineFirst, 2022. https://doi.org/10.1080/15732479.2022.2045613

[39] American Concrete Institute, Committee 440 "Guide for the Design and Construction of Structural Concrete Reinforced with Fiber-Reinforced Polymer (FRP) Bars", Farmington Hills, MI, USA, 2015.

[40] Meseguer, A. "Fundamentals of Numerical Mathematics for Physicists and Engineers", John Wiley & Sons, 2020. ISBN 978 1 11942 567 0 https://doi.org/10.1002/9781119425762